Supplementary Information

Plasticization resistant crosslinked polyurethane gas separation membranes

Ali Pournaghshband Isfahani [ab], Behnam Ghalei [b], Kazuki Wakimoto [b], Rouhollah Bagheri [a], Easan Sivaniah *[b] and Morteza Sadeghi *[a]

[a] *Department of chemical engineering, Isfahan University of Technology, Isfahan 84156-83111, Isfahan, Iran; Email: m-sadeghi@cc.iut.ac.ir*
[b] *Institute for Integrated Cell-Material Sciences (iCeMS), Kyoto University, 606-8501 Kyoto, Japan; Email: esivaniah@icems.kyoto-u.ac.jp*

1. Experimental method

1.1. Polymer synthesis

An excess amount of IPDI was slowly added to the dried pluronic-L61 at 80°C under N_2 atmosphere, following with two drops of DBTDL catalyst to obtain a macrodiisocyanate prepolymer. DBTDL organotin catalyst is a relatively stable tin-based catalysts for synthesis of polyurethane.[1, 2] After 2 h, an exact amount of the chain extender, 3,5-diamino benzoic acid (DABA), was added for equimolar adjustment of the NCO:OH ratio (Fig.S1). In our previous publications, it was shown that diamine chain extenders are preferred to synthesize PU membranes with high gas separation performance since it offers a free acid functionality within the hard segments of PU for further cross-linking.[3, 4] All synthesized PUs were precipitated and washed with methanol/water (50/50 vol.%) to remove any residual monomer and/or low molecular weight PU chains, and kept in vacuo at 70°C before using. The molar ratio of PTMG: IPDI: DABA was 1:3:2.

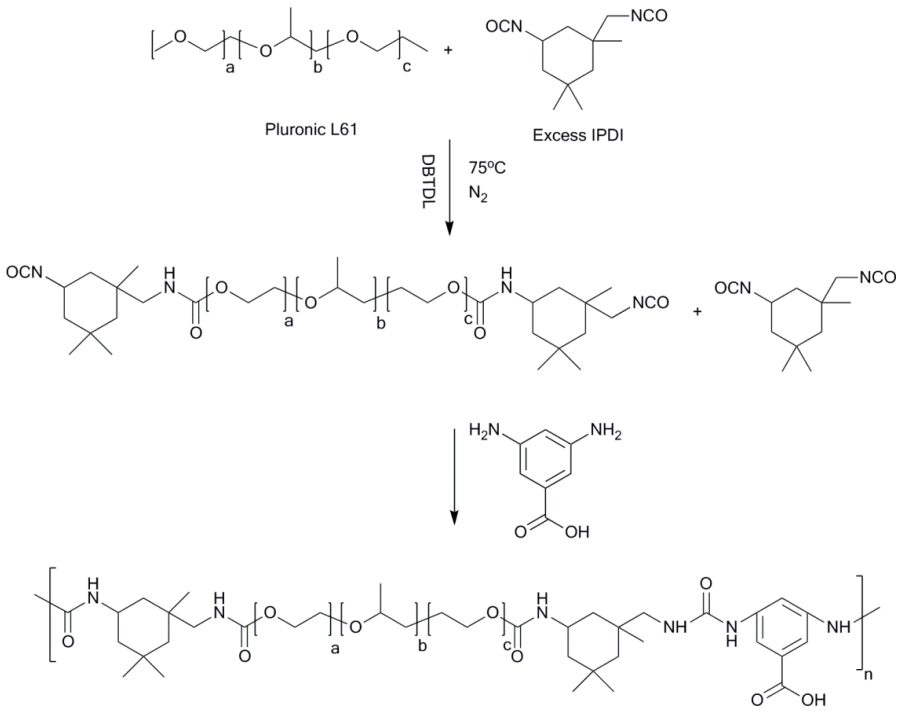

Fig. S1 Representation of two step polymerization of PUs and chemical structures

Supplementary Information

1.2. Membrane fabrication

Thick film membrane. Polyurethane thick film membranes were prepared by solution casting and thermal phase inversion method. The synthesized acyl chloride PU was dissolved and an excess amount (70 times stoichiometric) of the crosslinking agent was added for further reaction. Then, the 10g solution (5wt.%) was dissolved in NMP and directly casted in the Teflon petri dish (Ø=5cm) at room temperature and kept at 80^{o}C for 24 h for crosslinking reaction and evaporation of the solvent, simultaneously. This was followed in the vacuum oven to remove any residual solvent at 90^{o}C for 24h. The thickness of the membranes was measured by a micrometer gauge to be around 50 to 60 µm.

Thin film composite. An active coating layer on a highly permeable substrate is widely accepted concept for thin film membrane preparation. A thin film composite (TFC) membrane is attractive for the petroleum and chemical industries due to high permeability and versatility for module fabrication. α-alumina support, because of its high thermal stability and versatility with different solvents, was employed as the substrate material to fabricate the PU thin film membranes. The surface of α-alumina substrate was modified by γ-alumina solution to reduce the pore size configuration, preventing the penetration of polymeric solution through the pores. Pristine PU and XPU-HDA solutions (1 wt.%) were spun on the alumina substrate by spin coating machine with the spin rate of 2000 rpm and to prepare a homogenous bubble free film, the spun TFC immediately placed in a closed dish to prevent the swift evaporation.

1.3. Gas permeability measurement

The gas permeability values of the PU membranes were determined using a time lag apparatus (constant volume method) built from a stainless steel 25 mm filter holder (Millipore XX4502500) (effective area = 2 cm^2) equipped with a gas and vacuum line. A schematic representation of the gas separation system is shown in scheme 1. The pressure and temperature changes data were collected by absolute pressure sensor (Keller PAA 33X). All gases (CO_2, C_2H_6, H_2, CH_4, and N_2) were tested in triplicate at 35^{o}C and different pressure. Gas transports through the dense membranes are assumed to follow the diffusion-solution mechanism, where the relationship between permeability (P_i), diffusivity (D_i), and solubility (S_i) of gas species "i" can be described by equation S1 [5]:

$$P = DS \quad \text{(S1)}$$

The gas permeability depends on the mobility and diffusivity of the gas through the membrane, and the interaction between the membrane and permeant species (i.e. solubility).

The permeability of gas "i" (P_i) is calculated by equation S2:

$$P_i = J_i \frac{l}{\Delta p} = 10^{10} \frac{273.15}{76} \frac{V}{AT} \left(\frac{dp}{dt}\right) \frac{l}{\Delta p} \quad \text{(S2)}$$

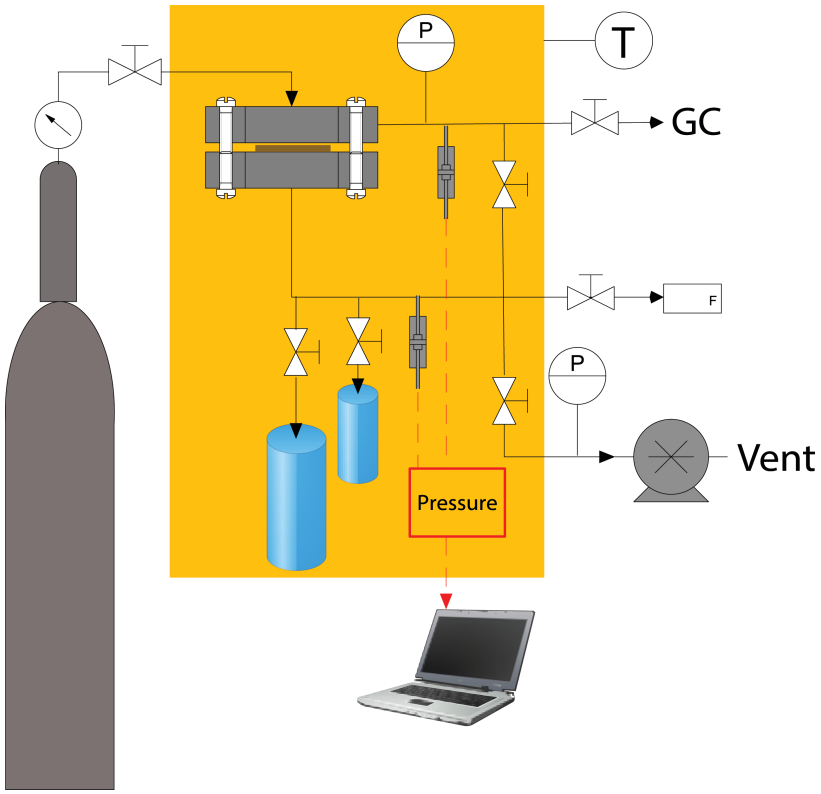

Scheme 1 **Schematic diagram of pure and mixed gas permeation apparatus.** P: pressure gauge or transducer; T: temperature controller; F: bubble flowmeter; V_1 and V_2: volume of gas sample cylinder 1 and 2 respectively; The membrane cell is placed in a temperature controlled box. In this study, the gas permeation was performed at room temperature of 35°C.

In the equation, J_i is the flux of gas "i"; Δp is the pressure difference across the membrane; l is the membrane thickness; $\left(\frac{dp}{dt}\right)$ is the steady-state slope of the permeate pressure versus t curve; V, A, and T are the permeate volume, the membrane area, and the temperature. The permeance (Q) is another definition of gas transport rate for the gas membrane application. The permeance is referred to as pressure normalized flux, quantifying the productivity of asymmetric or thin film composite membranes, while the permeability is employed for dense films. Units for the permeability are mol m m^{-2} s^{-1} Pa^{-1} or barrer, where barrer = 10^{-10} cm^3 (STP) cm cm^{-2} s^{-1} $cmHg^{-1}$. The relation of permeability to permeance is P = Ql. Units for the permeance are mol m^{-2} s^{-1} Pa^{-1} or Gas permeation Units (GPU), where 1 GPU equals to 10^{-6} cm^3 (STP) cm cm^{-2} s^{-1} $cmHg^{-1}$.

The diffusivity of gas "i" (D_i) can be determined separately from the time-lag (θ), which is the intercept on the t axis by extrapolating the slope of the linear portion of the p vs. t plot back to the time axis. This intercept can be related to D_i by equation S3:

$$D_i = \frac{l^2}{6\theta} \qquad \text{(S3)}$$

Supplementary Information

The ideal selectivity (αi/j) of the more permeable gas "i" to the less permeable gas "j" is simply defined by the ratio of gas permeabilities (equation S4), which can be written as the product of the diffusivity and solubility selectivities.

$$\alpha_{i/j} = \frac{P_i}{P_j} = \frac{D_i}{D_j}\frac{S_i}{S_j} \quad \text{(S4)}$$

The mixed gas separation of the membranes was measured at 35°C using the constant flow method with certified gas mixtures of CO_2/N_2 (50/50, 30/70, 18/85 vol.%) and CO_2/CH_4 (50/50 vol.%) at different upstream pressures (up to 20 bar). This method provides an easy comparison to the pure gas data to clarify the mixed gas conditions on the permeability and selectivity. The stage cut was set 2000 ml min^{-1} to ensure the residue gas composition on the membrane surface was equal to that of the feed gas. The gas compositions were analysed by a gas chromatograph machine (GC-2014, Shimadzu, Japan). The separation factor was calculated by:

$$\alpha_{i/j} = \frac{y_i / y_j}{x_i / x_j} \quad \text{(S5)}$$

where y and x are the mole fractions in the permeate and feed, respectively. The mixed gas permeability was calculated using: [6]

$$P_i = J_i \frac{l}{\Delta p} = 10^{10} \frac{273.15}{76} \frac{Vl}{AT} \left(\frac{dp}{dt}\right) \frac{y_i}{x_i \Delta p} \quad \text{(S6)}$$

where y_i and x_i are the mole fraction of the gas components in the permeate and feed streams.

2. FTIR characterization

The FTIR spectra of some synthesized PUs are shown in Fig.3 (a). The positions of the bands characteristics to the functional groups are very similar in all samples, but the differences concerning the band intensities in the C=O (1600-1800 cm^{-1}) region are noticed. The band observed at 1100 cm^{-1} is assigned to the anti-symmetric stretching vibrations of the C-O-C group, which was also reported for pure PTMG elsewhere [7]. There should be other bands, related to alkoxy oxygen of urethane groups at 1080 cm^{-1} display the characteristics of C-O-C, and a shoulder attributed to the hydrogen bonding interactions between NH and ether C-O-C groups at 1070 cm^{-1}, [8] which are difficult to distinguish in this work.

The absence of NCO peak at 2250 cm^{-1} suggests the completion of the PU synthesis reaction. A broad peak at 3200-3600 cm^{-1} assigns to the vibration of –OH and –NH groups from the DABA moiety and urethane functional groups, respectively. Furthermore, the analysis of the C=O stretching vibration (1800-1600 cm^{-1}) revealed the phase separation of the soft and hard segments. The N-H groups in PUs provide hydrogen bonds with strong proton acceptor functional groups in (i) urethane C=O group and (ii) ether C-O-C group in the soft segments.[3] The type and strength of these hydrogen bondings could be identified by the differences in the intensity and wave number shifts in double peaks at 1800-1600 cm^{-1}. The peak at lower frequency (around 1620 cm^{-1} for urea and around 1680 cm^{-1} for urethane) corresponds to the bonded carbonyl groups whilst the

peak appearing at higher frequency (around 1700 cm^{-1} and 1720 cm^{-1} for urea and urethane groups, respectively) refers to free carbonyl groups. As illustrated in Fig.3(a), the intensity of the bonded carbonyl bands in the XPUs increased and shifted to lower frequency, while the free carbonyl peak almost diminished. This observation indicates more hydrogen bonding between urethane carbonyl groups and the urethane NH groups, inferring more phase separation between the hard and soft segments. The phase separation can be characterized by the hydrogen bonding interactions between the hard-hard and hard-soft segments, that is usually evaluated by the following relation: [9]

$$\mathrm{HBI} = \frac{A_{C=O,bonded}}{A_{C=O,free}} \quad \text{(S7)}$$

where $A_{C=O,bonded}$ and $A_{C=O,free}$ are the absorbance of bonded and free carbonyls, respectively. The amount of phase separation of the synthesized PUs can be compared by this factor. In other words, increasing the amount of hydrogen bonding between the NH groups and carbonyl groups in the hard segment results more phase separation and higher hydrogen bonding index (HBI). The amount of HBI for prepared samples is shown in Table S1. Higher HBI for XPUs is predictable since the phase separation rate can easily be explained by crosslinking occurred in the media. By crosslinking the PUs, the crosslink agents forced the chains in hard segments to keep them near together. These new bonds prevent the chains to mix with soft segment chains. As a result, the largest HBI was observed for XPU-ODA material with the highest crosslinking density.

3. Diffusivity and solubility

The gas permeability is contributed by both diffusivity and solubility according to the solution-diffusion model. The variations of diffusivity and solubility coefficients for representative samples are calculated by the time-lag method (Eq. S1 and Eq. S3) and presented in Fig. S2(a) and S2(b). Gas diffusivity coefficient depends on the penetrant kinetic diameter, which confirms the existence of molecular sieving ability of the synthesized membranes. The C_2H_6 diffusivity is the lowest among the other tested gases due to its larger kinetic diameter. Interestingly, the apparent diffusivity of N_2 is larger than CO_2, though the N_2 kinetic diameter is larger than that of CO_2. The strong CO_2 sorption in PUs retards the CO_2 diffusion, which was observed in our previous work as well.[4] However, time lag method has some limitations in determining the diffusion coefficients of small gas molecules such as H_2, with high amounts of diffusivity.[10-12] The gas diffusivity drops greatly for crosslinked membranes, where increasing stiffness and chain packing obstructed the gas transport throughout the membrane. The calculated gas solubility coefficient correlates well (Fig. S2(b)). with the critical temperature of the gas molecules, following the order of: C_2H_6 (305.3 K)> CO_2 (304.2 K)> CH_4 (190.9K)> N_2(126.3K)> H_2 (33.2 K).[13] The decrease in chain mobility for crosslinked membranes led to lower gas sorption, which results a decline for CO_2/H_2 selectivity. This effect was also reported elsewhere for other crosslinked membranes. [14, 15]

Supplementary Information

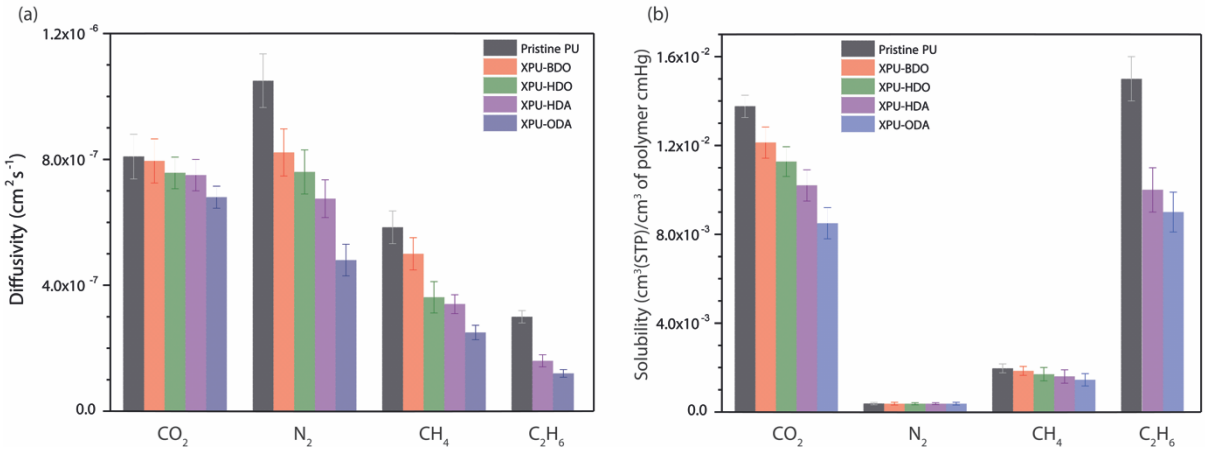

Fig. S2 Variations of (a) gas diffusivity and (b) solubility in different XPU membranes measured at 35°C and 4 bar.

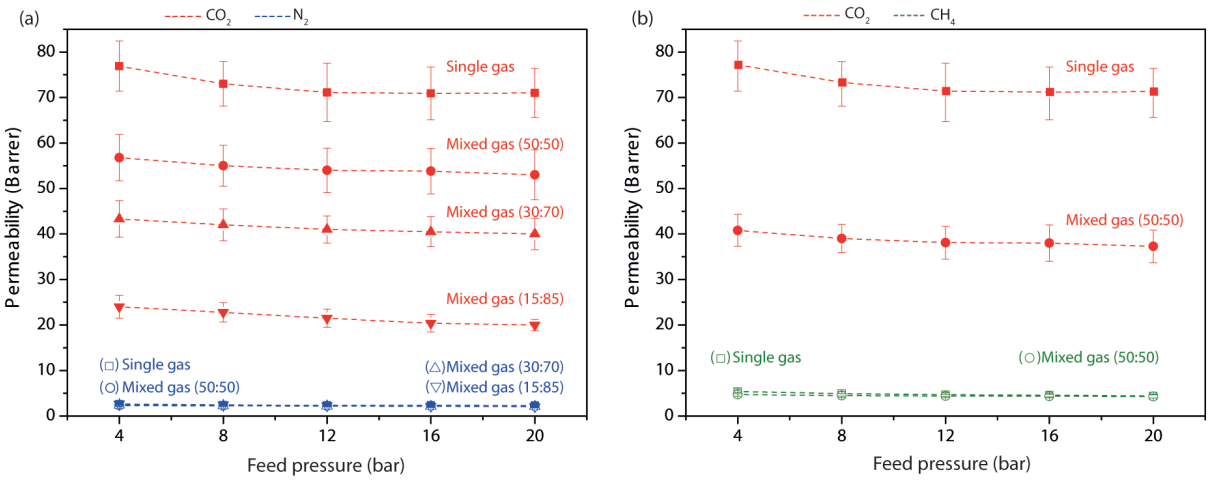

Fig. S3 Pure gas and mixed gas permeability of CO_2, N_2 and CH_4 of XPU-HDA membrane as a function of feed pressure at 35°C for (a) three different CO_2/N_2 composition (50/50, 70/30, 10/90 vol.%), and (b) CO_2/CH_4 (50/50 vol.%)

Table S1. Thermal and morphological properties of pristine PU and crosslinked PU membranes

Sample	T_g (°C)	$T_{50\%}$ (°C)	$d_{spacing}$ (Å)	HBI
Pristine PU	-50.5	357	4.8	0.86
XPU-BDO	-53.3	399	4.6	1.03
XPU-HDA	-54.5	441	4.5	2.40
XPU-ODA	-58.4	455	4.4	2.90

Supplementary Information

Table S2. Gas transport properties of pristine PU and crosslinked PU membranes at 35°C

Sample	Pressure (bar)	Permeability (barrer)				Selectivity		
		CO_2	H_2	CH_4	N_2	CO_2/N_2	CO_2/H_2	CO_2/CH_4
Pristine PU	2	130.2±11.5	28.3±2.4	13.9±1.0	4.7±0.3	27.7±3.0	4.6±0.6	9.4±1.1
	4	111.3±7.8	27.3±2.0	11.5±1.2	4.0±0.4	27.8±3.4	4.1±0.4	9.7±1.2
	6	100.5±8.4	26.4±2.1	10.2±1.2	3.5±0.3	28.7±3.4	3.8±0.4	9.9±1.4
	8	94.3±8.1	25.9±1.8	9.2±0.8	3.3±0.2	28.6±3.0	3.7±0.4	10.3±1.3
	10	94±7.7	25.1±2.3	8.9±0.9	3.2±0.4	29.6±4.4	3.7±0.5	10.6±1.4
XPU-BDO	2	105.7±8.1	27.5±2.1	11.1±1.0	3.7±0.2	28.6±2.7	3.8±0.4	9.5±1.1
	4	96.4±7.2	26.8±2.3	9.0±0.9	3.1±0.3	31.1±3.8	3.6±0.4	10.7±1.3
	6	90.1±7.3	24.8±1.9	8.3±0.7	2.8±0.3	32.2±4.3	3.6±0.4	10.9±1.3
	8	87.0±6.9	24.6±1.6	7.9±0.5	2.7±0.2	32.2±3.5	3.5±0.4	11.0±1.1
	10	84.0±6.6	24.7±2.0	7.4±0.6	2.6±0.2	32.3±3.6	3.4±0.4	11.6±1.3
XPU-HDO	2	90.2±8.1	27.0±2.5	7.6±0.7	3.2±0.3	28.2±3.7	3.3±0.4	11.9±1.5
	4	85.3±7.7	26.4±2.5	6.2±0.8	2.9±0.2	29.4±3.3	3.2±0.4	13.7±2.1
	6	79.4±6.8	25.3±2.1	5.6±0.6	2.6±0.2	30.5±3.5	3.1±0.4	14.2±1.9
	8	74.0±6.8	24.7±2.3	5.0±0.4	2.4±0.2	30.8±3.8	3.0±0.4	14.8±1.8
	10	72.7±6.4	24.5±1.9	4.8±0.5	2.4±0.3	30.3±4.6	2.9±0.3	15.1±2.1
XPU-HDA	2	81.5±7.0	26.9±2.5	5.9±0.6	2.8±0.2	29.1±3.3	3.0±0.4	13.8±1.8
	4	76.9±5.4	26.0±2.8	5.4±0.5	2.6±0.2	29.6±3.1	3.0±0.4	14.2±1.6
	6	75.2±6.8	24.6±2.3	5.2±0.4	2.5±0.2	30.1±3.6	3.0±0.4	14.5±1.7
	8	73.0±6.1	24.4±2.0	4.9±0.4	2.4±0.2	30.4±3.6	2.9±0.4	14.9±1.7
	10	71.2±6.5	24.3±1.8	4.7±0.4	2.3±0.2	31.0±3.9	2.9±0.3	15.1±1.9
XPU-ODO	2	65.0±6.0	24.5±2.0	4.7±0.4	2.2±0.2	29.5±3.8	2.7±0.3	13.8±1.7
	4	62.5±5.8	24.2±2.1	4.5±0.5	2.1±0.1	29.9±3.3	2.6±0.3	13.9±2.0
	6	61.7±5.2	24.1±2.3	4.3±0.4	2.0±0.1	30.9±3.0	2.6±0.3	14.3±1.8
	8	60.6±4.8	24±2.5	4.2±0.4	2.0±0.2	30.3±3.9	2.5±0.3	14.4±1.8
	10	59.5±5.1	23.9±1.8	4.0±0.4	1.9±0.1	31.3±3.1	2.5±0.3	14.9±2.0
XPU-ODA	2	59.7±5.1	23.8±2.0	4.2±0.4	2.0±0.1	29.9±3.0	2.5±0.3	14.1±1.8
	4	57.9±6.1	23.8±1.9	4.1±0.3	1.9±0.1	30.5±3.6	2.4±0.3	14.1±1.8
	6	56.2±4.8	23.6±1.7	3.9±0.3	1.8±0.1	31.2±3.2	2.4±0.3	14.4±1.7
	8	55.5±4.6	23.6±1.8	3.9±0.3	1.8±0.1	31.8±3.1	2.4±0.3	14.6±1.6
	10	55±4.8	23.5±1.9	3.7±0.2	1.7±0.1	32.6±3.4	2.3±0.3	15.0±1.5

Supplementary Information

References

1. M. Szycher, *Szycher's handbook of polyurethanes*, CRC press, 1999.
2. A. B. Ferreira, A. Lemos Cardoso and M. J. da Silva, *ISRN Renewable Energy*, 2012, **2012**, 1-13.
3. M. Sadeghi, M. A. Semsarzadeh, M. Barikani and B. Ghalei, *Journal of Membrane Science*, 2010, **354**, 40-47.
4. A. P. Isfahani, B. Ghalei, R. Bagheri, Y. Kinoshita, H. Kitagawa, E. Sivaniah and M. Sadeghi, *Journal of Membrane Science*, 2016, **513**, 58-66.
5. R. W. Baker, in *Membrane Technology and Applications*, John Wiley & Sons, Ltd, 2004, pp. 15-87.
6. P. Tin, T. Chung, Y. Liu, R. Wang, S. Liu and K. Pramoda, *Journal of Membrane Science*, 2003, **225**, 77-90.
7. J. Bandekar and S. Klima, *Journal of Molecular Structure*, 1991, **263**, 45-57.
8. L. Bistričić, G. Baranović, M. Leskovac and E. G. Bajsić, *European Polymer Journal*, 2010, **46**, 1975-1987.
9. R. Seymour, G. Estes and S. Cooper, *Macromolecules*, 1970, **3**, 579-583.
10. J. Crank, *The mathematics of diffusion*, Oxford university press, 1979.
11. Y. Rogan, R. Malpass-Evans, M. Carta, M. Lee, J. C. Jansen, P. Bernardo, G. Clarizia, E. Tocci, K. Friess and M. Lanč, *Journal of Materials Chemistry A*, 2014, **2**, 4874-4877.
12. N. Morlière, J.-P. Corriou, E. Favre and D. Roizard, *Desalination*, 2002, **144**, 109-113.
13. Q. Song, S. K. Nataraj, M. V. Roussenova, J. C. Tan, D. J. Hughes, W. Li, P. Bourgoin, M. A. Alam, A. K. Cheetham, S. A. Al-Muhtaseb and E. Sivaniah, *Energy & Environmental Science*, 2012, **5**, 8359-8369.
14. J. D. Wind, C. Staudt-Bickel, D. R. Paul and W. J. Koros, *Macromolecules*, 2003, **36**, 1882-1888.
15. A. M. Hillock and W. J. Koros, *Macromolecules*, 2007, **40**, 583-587.